International Journal for Innovative Engineering and Management Research
PEER REVIEWED OPEN ACCESS INTERNATIONAL JOURNAL
www.ijiemr.org

COPY RIGHT

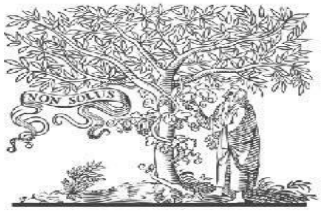

ELSEVIER SSRN

2023 IJIEMR. Personal use of this material is permitted. Permission from IJIEMR must be obtained for all other uses, in any current or future media, including reprinting/republishing this material for advertising or promotional purposes, creating new collective works, for resale or redistribution to servers or lists, or reuse of any copyrighted component of this work in other works. No Reprint should be done to this paper, all copy right is authenticated to Paper Authors

IJIEMR Transactions, online available on 31st Mar 2023. Link :http://www.ijiemr.org/downloads.php?vol=Volume-12&issue=Issue 03

10.48047/IJIEMR/V12/ISSUE 03/101

Title **A VOLTAGE CONTROL APPROACH FOR GRID-INTEGRATED SOLAR PV SYSTEMS USING IGI**

Volume 12, ISSUE 03, Pages: 695-705

Paper Authors
Dr. P. Lakshman Naik, D.Pragathi, D. Mahesh, CH. Syam Prakash Reddy, A. Deepak

USE THIS BARCODE TO ACCESS YOUR ONLINE PAPER

To Secure Your Paper As Per UGC Guidelines We Are Providing A Electronic Bar Code

International Journal for Innovative Engineering and Management Research
PEER REVIEWED OPEN ACCESS INTERNATIONAL JOURNAL
www.ijiemr.org

A Voltage Control Approach for Grid-Integrated Solar PV Systems Using IGI

Dr. P. Lakshman Naik, Faulty, Department of EEE,
Vasireddy Venkatadri Institute of Technology, Nambur, Guntur Dt., Andhra Pradesh.

D.Pragathi, D. Mahesh, CH. Syam Prakash Reddy, A. Deepak
UG Students, Department of EEE,
Vasireddy Venkatadri Institute of Technology, Nambur, Guntur Dt., Andhra Pradesh.
E-Mail ID: pragathidammati@gmail.com
maheshdarshanam1434@gmail.com
saireddychalla60@gmail.com
deepakamarthala905@gmail.com

Abstract:

Voltage and power quality management are the primary components for regulating grid integrated voltage source converters (VSC) during abnormal grid disturbances. This Project offers a distinct control method for controlling a grid-connected solar photovoltaic (PV) system that makes use of an IG integrater. The topology of a three-stage and single stage is investigated. The former purpose is to maintain Photo voltaic power flowing to the power grid although when the system is experiencing irregular oscillations. Normally, the system provides Unity power factor (UPF). Despite this, when the grid voltage varies, reactive power injection keeps the PCC voltage profile within the permissible limits. Moreover, LVRT functioning occurs in the presence of substantial voltage sags.During the night, when there is no PV generation, the VSC and DC link capacitor act as a distribution static compensator, enhancing system usage (DSTATCOM). In contrast to usual control approaches, the power quality of the system is not reduced. The successes of the control are demonstrated through simulation implementation.A comparison with state-of-the-art processes is also emphasized, illustrating the utility of the supplied control.

Keywords:Power Quality, Solar Photo Voltaic Generation, LVRT,Voltage Regulation, IG Integrator,

I. Introduction:

The enhancement of solar PV systems tends todevelop in R&D of control of grid embedded with SPEC systems.

Unfortunately, it has been resulted in more number of power quality difficulties in these system. The coming introduction of PE and Abnormal loads systems has added to the pressure.As a result,the VSC is importance to connect to the Grid.To solve the challenges, several mechanisms have been created. The commonly utilized kind of control is called VCC. It is based on the Di-Quadratic Zero transformation, which requiresto use The PLLwhichj is Known As Phase Locked Loop.to achieve grid contemporise. There have been several research on PLLs with diverse topologies

and properties [2],[3] describes a multi-harmonic PLL based on decoupling Cell so,that can synchronize quickly at distorted voltages. Moreover, [4] it describes the combination of DSOGI and

PLL. Moreover, [5] proposes an ISOGI-PLL for microgrid control.

These approaches are important for achieving injecting of reactive power and operation of UPF.Even so, at lower frequencies, it causes execution instability and provides negative accumulative resistance [6][7]. The deterioration in power quality complicates execution. As a result, a control mechanism that does not rely on PLL is required for the grid VSC's steady and optimal operation.To overcome these issues, several control mechanisms have been proposed. [8] defines model predictive control (MPC), which predicts future switching states. Because the information for the next prediction is provided ahead of time, the operationability is sufficient for steady-state conditions. But, with dynamic changes, it loses its benefit of speed and incurs a high computational cost. In addition, [9] includes a least mean fourth (LMF)-based control that produces outstanding results but lacks precision due to order four optimization.If the inaccuracy in the governing equation of a dynamic loading operation is smaller than one, the algorithm's weights take a long time to converge to the correct value. [9] describes control ytechniques developed on the Kalman-filter (KF) that are used to improve power quality through the correction and prediction process. Its improved representations, such as expanded KF, are also available in [11] to expand its operational capabilities. However, because the derivative property is used in the calculation, it causes a significant computational strain on the system and requires additional memory for storage, resulting in an increased overload on the processor.

The second order generalized integrator (SOGI) [12] is a well-known and widely employed control technique. It has an edge over others due to its simplicity and ease of implementation. When lower order harmonics and DC offset are present, however, its performance degrades substantially. Moreover, its lack of dynamic capabilities exacerbates the issue. [13] describes a SO-SOGI-based control technique that does not work well in highly distorted grid conditions. [13] describes a modified SOGI to overcome these difficulties. Yet, its implementation causes operational trouble since computations need familiarity with the preceding dominant frequency response. There are also other variations available, such as the fifth order generalized integrator (FOGI) [15].Growing computing complexity, on the other hand, places a strain on a low-cost Processor. Furthermore, due to the widespread usage of distributed energy resources (DERs) in current power grid networks, the PCC voltage is vulnerable to significant variations as a result of breakdowns. This might cause the system to crash. According to IEEE standard 1547a [16], DERs can offer PCC voltage support by managing the apparent power flow in the grid. The recommended voltage restricts differ depending on the codes of

International Journal for Innovative Engineering and Management Research
PEER REVIEWED OPEN ACCESS INTERNATIONAL JOURNAL
www.ijiemr.org

grid. Yet, in this case, the limitations are set at 0.9 per unit to 1.1 per unit [11].

Undervoltage occurs when the voltage at PCC falls below 0.9 pu. It affects system reliability, power performance. This might results substantial problems with grid-connected PV-systems, leading them to trip and further restrict use. This might cause it to fail unexpectedly. When voltage sags,reactive-power is fed into the system network to help until the decreased voltage at the PCC reachescontinuous operating boundaries.

Yet, reactive-power is affected by system rating and voltage sag. If the PCC voltage falls below a specific level, the reactive power needed to sustain the system excxeeds the system's rating. In such instances, reactive powerinjected in compliance with grid norms, resulting in a low voltage ride through (LVRT) operation [11][17].

The key aims in development of the control are as follows.

•Create an generalized integrator (IGI) control system to send PV power to the PCC and feed the grid.

• Demand-based regulation of active, reactive electricity provided into grid networkduring anomalous grid fluctuations.

• Unlike past systems, this control uses reactive power injection to provide voltage support during undervoltage.

• It allows for a low voltage ride through during periods of acute undervoltage (LVRT).

• When there is no solar irradiation throughout the night,system acts as a static (DSTATCOM).

• During all of these procedures, the system's power quality is kept well within limits.

II. SCHEMATIC SYSTEM

As shown in Fig.1[1], a single stage three phase design is used here, with a single (DC-AC)converter for both maximum power point tracking (MPPT) and power conversion. This minimise overall system loss and requires less space than a two-stage design [18]-[21]. A voltage source converter (VSC) in a single stage 3-Φ architecture delivers the Photo voltaic power to the grid, ensuring maximum power point tracking (MPPT) of the Photo voltaic panel.The MPPT employs the incremental conductance (InC) approach. To reduce VSC current ripples, interfacing inductors (Li) are also used.

During normal operation, Photo voltaic power is sent to the grid at a power factor of one; during grid fluctuations, reactive power is supplied to sustain voltage ofr PCC; and during at night, the system acts as a Distribution STATCOM.

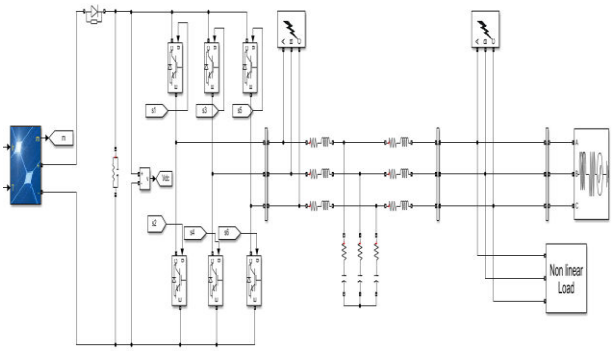

Fig.1.Single stage 3-phase gridinterfaced solarPVsystem

International Journal for Innovative Engineering and Management Research
PEER REVIEWED OPEN ACCESS INTERNATIONAL JOURNAL
www.ijiemr.org

III. IG INTEGRATOR-BASED CONTROL APPROACH

In Fig. 2[1], the IGI (Interweaved Generalized Integrator) control is employed to manage the single stage system and provide switching pulses for the VSC.

Grid currents (iga, igb, igc), load currents (iLa, iLb, iLc), DC link voltage (VDC), PCC voltages (vpcc a, vpcc b, vpcc c), and PV array voltage and current (Vpv and Ipv) are all important control inputs.

• Calculation of the reference reactiveB C currents for undervoltage support as well as LVRT.

• Creating switching pulses.

These procedures are outlined below[1].

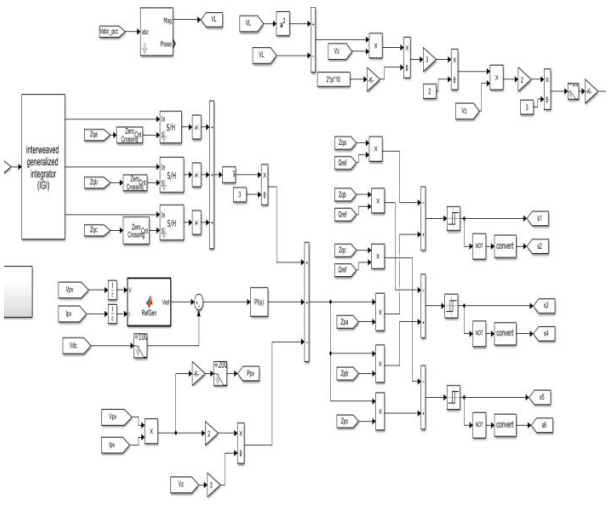

Fig.2.IGIbasedcontroltechnique

1. Functioning of the IGI Filter:

The IGI filter is used at the PCC to estimate The requirements of the load (Fig. 2). The load currents are measured and sent into the filter, that calculates the components of load currents. The IGI has 4 integrators. It is made up of appropriate cross-feedback network connection that are utilized to mitigate DC components, harmonics, and subharmonic component, as well as eliminate oscillatory distortion and damping. The load currents (iLabc) are

control inputs that are translated into co-mponents using Clarke's transformatin.

As inputs, components (α) and (β) are sent into the filter.

Here, $\xi 1, \xi 1', \psi 1, \psi 2, \psi 1', \psi 2', \varepsilon, \varepsilon' and\ \zeta$ consider as the input signal of a filters, while, $\omega n, \varphi, H(s)\ and\ \rho$are the gain for amplification, rectification of errors, as well as damping, delay reduction, which give the $\xi 2\ and\ \xi 2'$is the essential components of load current.

All variables are depicted in Fig. 2 and are specified in below.

α and β are the components of input.ψ1, ψ1' are the totals of the outside loops.

Ψ2,Ψ2' are the totals of the inside loops.

Φ will be the erroe amplification gain.ε,ε' are the internal signal of error.ρ is the coefficient of delay mitigationof the integrator.ωn is the cutoff frequency.

Ωξ1,ωξ1'are belongs to the error loop.ωξ2,ωξ2'are the loops of coupling.ξ1 and ξ2are the filter's output, which makes up the majority of the input.

The following are the prime equations for the filter[1].

The load current components in αβ frame will be ξ2, ξ2'Their values in the frame of abc are derived by applying the inverse

International Journal for Innovative Engineering and Management Research
PEER REVIEWED OPEN ACCESS INTERNATIONAL JOURNAL
www.ijiemr.org

Clarke's transformation (iLabc). Internal parametric values are to be chosen depending on the damping.

$$\psi_1 = \chi_a - \xi_2 - H(s)\xi_2 \ , \ \psi_2 = \psi_1 - \xi_1 - H(s)\xi_1 \quad (1)$$

$$\varepsilon = \psi_2\varphi - \xi_1'\,\omega \ , \ \xi_1 = \frac{\varepsilon}{s+\rho} \Rightarrow \frac{\psi_2\varphi - \xi_1'\,\omega}{s+\rho} \quad (2)$$

$$\xi_1 = \frac{\psi_1\varphi - H(s)\xi_1\varphi - \xi_1\varphi - \xi_1'\,\omega}{s+\rho} \quad (3)$$

$$\xi_1 = \frac{\chi_a\varphi - H(s)\xi_2\varphi - \xi_2\varphi - H(s)\xi_1\varphi - \xi_1\varphi - \xi_1'\,\omega}{s+\rho} \quad (4)$$

Therefore, $\xi_2 = \frac{\xi_1\omega_n - \xi_2'\omega}{s+\rho}$ (5)

Similarly, $\xi_1' = \frac{\chi_b\varphi - H(s)\xi_2'\varphi - \xi_2'\varphi - H(s)\xi_1'\varphi - \xi_1'\varphi + \xi_1\omega}{s+\rho}$ (6)

Therefore, $\xi_2' = \frac{\xi_1'\omega_n + \xi_2\omega}{s+\rho}$ (7)

the amplification and error corrrection as shown in figure2.

2.Unit Templates Estimate:

The estimation of unit templates can be done by using PCC voltages.It is important to note that these three numbers—"Vo" stands for maximum value of the coventional grid voltage is 1 per unit, "VL" is the lower limit of maximum value of the PCC voltage, and "VZ" is the maximum value of the instant PCC voltage—are essential for control before moving on. The representation of each of these variables is shown in the Figure. 3[1].

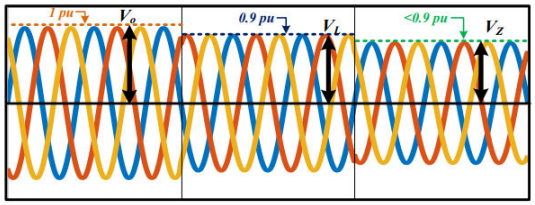

Figure 3: 3- phase voltage waveform and their maximum amplitudes VO, VL, VZ.

Here, it is established that the instantaneous peak amplitude (VZ) of the PCC voltage is,

$$V_Z = \sqrt{\left(v_{pcc\_\alpha}\right)^2 + \left(v_{pcc\_\beta}\right)^2} \quad (8)$$

where the PCC voltages for the specified frame are Vpcc_ and Vpcc_. The instantaneous p.u voltage of PCC and minimum limit of minimum amplitude are computed as follows:

$$V_{pu} = \frac{V_Z}{V_o} \quad (9)$$

$$V_L = 0.9 \times V_o \quad (10)$$

Unit template evaluations range from (8)

$$\begin{bmatrix} z_{pa} \\ z_{pb} \\ z_{pc} \end{bmatrix} = \frac{1}{V_Z} \times \begin{bmatrix} v_{pcc\_a} \\ v_{pcc\_b} \\ v_{pcc\_c} \end{bmatrix} \quad (11)$$

Using (11) we can derive the unit templates of quadrature components as follows:

$$\begin{bmatrix} z_{qa} \\ z_{qb} \\ z_{qc} \end{bmatrix} = \frac{1}{2\sqrt{3}} \begin{bmatrix} 0 & -2 & 2 \\ 3 & 1 & -1 \\ -3 & 1 & -1 \end{bmatrix} \times \begin{bmatrix} z_{pa} \\ z_{pb} \\ z_{pc} \end{bmatrix} \quad (12)$$

3. Active Power Current Estimation:

The Photovoltaic electricity is supplied to the power grid side at a power factor of unity during standard grid operation. Reactive power thus equals 0.With the use of three parts [5], the currents of base grid signifying the active power are calculated.The load component, which meets the nonlinear load's power requirements at PCC, comes first. This requires a fundamental load current component. IG integrator control is utilized to extract it Figure.2. The maximum value of load current is calculated using sample and hold (S/H) circuit and a zero crossing detector (ZCD), which are activated by the components of quadrature of the unit templates. An

International Journal for Innovative Engineering and Management Research
PEER REVIEWED OPEN ACCESS INTERNATIONAL JOURNAL
www.ijiemr.org

evaluation of the active power currents of load component of reference is given based on the logic in Figure. 2.

$$\mu_{load} = \frac{\mu_a + \mu_b + \mu_c}{3} \quad (13)$$

The purpose of the dynamic feedforward term, according to the second assessment, is to increase the system's dynamic responsiveness to the varying solar irradiation that a real solar PV system encounters.

$$\mu_{pvg} = \frac{2 \times V_{pv} \times I_{pv}}{3 \times V_Z} \quad (14)$$

For the DC link voltage control, losses in VSC are also used. The DC voltageof the single stage architecture is equal to Vpv (VDC = Vpv). Hence, VDC ref = Vpv ref, where VDC ref is the base reference voltage output of MPPT algorithm and VDC ref is the reference voltage of the DC connection. and the measured DC link voltage is compared to this reference (ed = VDC ref VDC) before using a PI controller. It is shown as follows in Fig. 2:

$$\mu_{loss} = K_p(e_d) + K_i \int e_d(\tau) d\tau \quad (15)$$

Where Ki, Kp represent the integral and proportional gains of the PI controller, respectively.

Thus, the active power component of the peak value of the current in grid can be defined as,

$$\mu_{net} = \left(\mu_{loss} + \mu_{load} - \mu_{pvg}\right) \quad (16)$$

When this maximum value times, base active grid currents, unit templates—which reflect the active power that must be supplied to the grid—are created.

$$\begin{bmatrix} i_{pa}^* & i_{pb}^* & i_{pc}^* \end{bmatrix}^T = \mu_{net} \begin{bmatrix} z_{pa} & z_{pb} & z_{pc} \end{bmatrix}^T \quad (17)$$

The current indicated is used in calculation of total active power being sent to the grid (17).

$$P_{ref} = \frac{3}{2} \times \mu_{net} \times V_Z \quad (18)$$

4. Calculation of Current in Reactive Power:

Reactive power is delivered to maintain the grid in situations where there is a high reactive demand or a failure. The system's PCC voltage fluctuates in a number of ways. As a result, DERs are utilized to change the amount of power transferred into the grid so that the voltage profile working limits of 0.9 pu to 1.1 pu and so avoid undervoltage-related failures. This requirements' definition of the PCC voltage's acceptable safety range. To

achieve these restrictions, several undervo ltage techniques are utilized.If the voltage is less than the lower barrier (0.9 pu), reactive power is injected, eliminating the potentially harmful effects of voltage sag. To do this, basic PCC voltage is needed. A base reactive power is derived based on the sag's magnitude [21] after it has been detected.

$$Q_{ref} = \frac{3}{2}\left[\frac{V_L^2 - V_L \times V_Z}{\omega L_g}\right] \quad (19)$$

Where Lg is the line's inductance, and Fig. 3 shows all the variables. Input of this much reactive power will cause the PCC voltage to rise until the lower limit is reached. This approach is known as under-voltage support.

International Journal for Innovative Engineering and Management Research
PEER REVIEWED OPEN ACCESS INTERNATIONAL JOURNAL
www.ijiemr.org

The following are the calculated reference reactive currents:

$$\begin{bmatrix} i_{qa}^* & i_{qb}^* & i_{qc}^* \end{bmatrix}^T = \left(\frac{2}{3}\times Q_{ref}\times V_Z\right)\times\begin{bmatrix} z_{qa} & z_{qb} & z_{qc} \end{bmatrix}^T \quad (20)$$

During this operation, the following calculations are conducted about the reference active current:

$$\left.\begin{aligned} P_{\max} &= \sqrt{\left(\frac{3}{2}\times\mu_{net}\times V_Z\right)^2 - \left(Q_{ref}\right)^2}, \\ \text{if } P_{ref} > P_{\max} &\Rightarrow P_{ref} = P_{\max} \end{aligned}\right\} \quad (21)$$

Under the supply limit of active power, the updated maximum value of base active current is calculated as,

$$\mu_{net\_(new)} = (2\times P_{ref})/(3\times V_Z) \quad (22)$$

The data provided by are then used to determine the reference active current (18).

The amount of reactive power base on that must be supplied for voltage support may occasionally surpass the whole system rating. This algorithm changes to low voltage ride through operation to avoid this situation, needing only a significant amount of reactive power to be injected into the grid to maintain the system during the brief period of high voltage sag. The converter's required input of reference reactive power into the grid to carry out LVRT is calculated as follows [10],

$$Q_{ref} = \frac{3}{2}\times\left(\frac{S_t * V_L - S_t * V_Z}{V_o}\right) \quad (23)$$

In this circumstance, St is the highest apparent power. By introducing this quantity of reactive power into the system, the grid may be able to keep it running until the sag disappears. In order to maintain the power injection within the rating, a current limiting restriction is applied to the active power reference during voltage sags.

$$\left.\begin{aligned} P_{\max} &= \sqrt{S_t^{\,2} - Q_{ref}^{\,2}}, \\ \text{if } P_{ref} > P_{\max} &\Rightarrow P_{ref} = P_{\max} \end{aligned}\right\} \quad (24)$$

The peak value of reference active current is then calculated from (23) and reference active and reactive current are then calculated from (18) and (21).All steps may be seen in the flowchart in Fig. 4. Using this technique, one may ensure voltage support via LVRT and PCC undervoltage control.

5. Generating Switching Pulses:

Following are evaluations of the overall reference grid currents:

$$\begin{bmatrix} i_{ga}^* & i_{gb}^* & i_{gc}^* \end{bmatrix}^T = \begin{bmatrix} i_{pa}^* & i_{pb}^* & i_{pc}^* \end{bmatrix}^T + \begin{bmatrix} i_{qa}^* & i_{qb}^* & i_{qc}^* \end{bmatrix}^T \quad (25)$$

The difference between the coventional grid currents and the detected currents in grid is received by the current controller of hystersis, which it then employs to create the switching pulses of VSC.

IV. RESULT ANALYSIS:

Figure 5 For various grid configurations, the performance of the IGIintegrator-based control in Simulink is demonstrate d. Parameters offers detailed system and control settings.

The voltage grows till it approaches the 0.9pu limit.The injected reactive power is roughly 2.42 kVAr, which is pushed into the grid. This clearly shows how IGI works with undervoltage help.As shown in Fig. 5(b), the PCC voltage is dropped to 0.7 pu to demonstrate performance in the presence of significant voltage sag. If the

International Journal for Innovative Engineering and Management Research
PEER REVIEWED OPEN ACCESS INTERNATIONAL JOURNAL
www.ijiemr.org

reactive power calculated from (20) exceeds the system rating, undervoltage support cannot be performed; hence, the reactive power is estimated from (24) to perform LVRT. The reference active power is determined once the current limiting is imposed (25).

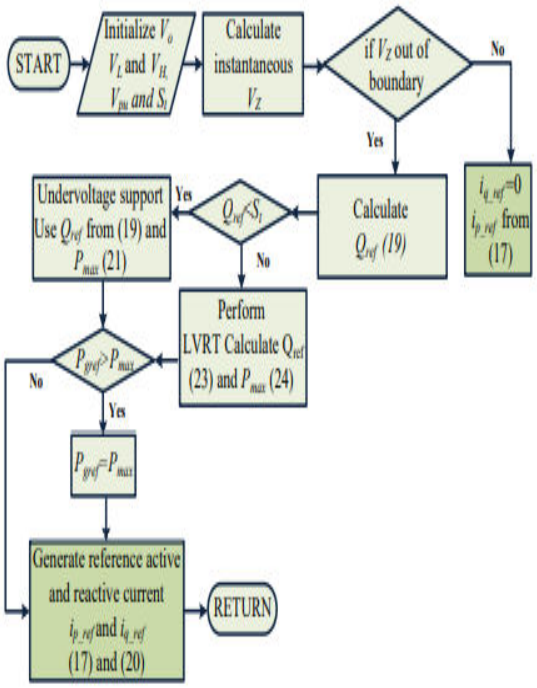

The active reference currents are computed using (25), (23) and (18), whereas the reactive reference currents are computed using (21). The total reference grid currents from (26) are then computed, followed by a low voltage ride through.In this location, the reactive power supplied into the grid is around 2.2kVAr. The Photo voltaic power is reduced somewhat to maintain thelimitation restriction of the current.

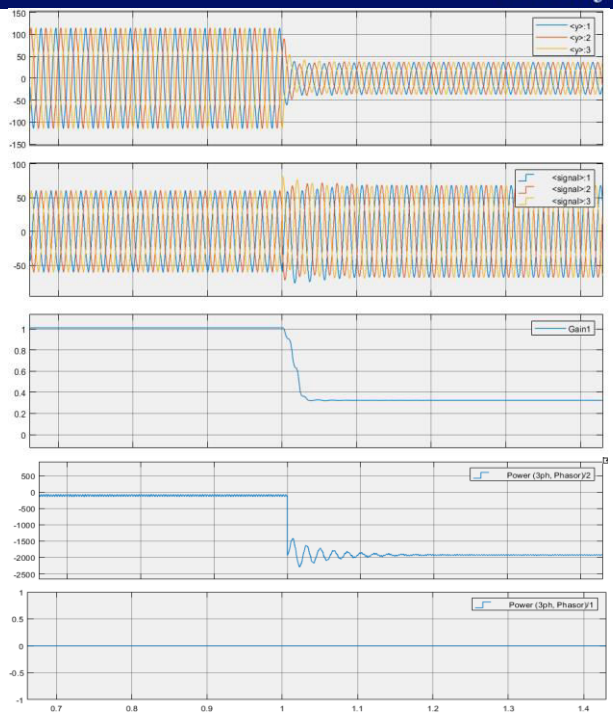

Fig: Simulation results

The responsiveness of the supplied IGIntegrator control are compared to the most used algorithms and VLLMS [23]. As seen in Fig., the results of the VLLMS degrades highly during load unbalancing in terms of oscillations. When compared to other algorithms, it performs poorly.In terms of performance, DSOGI, SO-SOGI, and MSOGI surpass VLLMS; nevertheless, their time settling is considerable. The current load is decreased, and one phase is shut off for 0.8s-1.1s.Itdepicts the peak value of the basic load current extraction (load).In terms of performance, the IGI control beats other methods. It reduces oscillations via highest value of the basic load current extraction (load)This emphasizes the usage of IGI control by demonstrating superior performance when compared to other cutting-edge approaches. The desired value is rapidly

reached with no deviations.It demonstrate how IGI control works when grid voltage changes. Undervoltage and overvoltage can occur on the grid. The control response is ensnared in phase a. The grid voltage (vpcca) is dropped, but the load current (iLa) and grid current (iga) are raised. The grid currents increases due to drop in PCC voltage and constant load impedence. The consistent DC connection voltage (VDC) demonstrates the control's endurance. To illustrate operation during an overvoltage circumstance, the grid voltage is raised. In this situation, the current in grid declines, the increase in load current then DC link voltage will remains constant.

VI. Conclusion:

Based on IGI control approach for this paper describes a single stage grid-interfaced solar pvsystem of energy conversion. The control is exposed to several anomalous grid circumstances while accounting for a nonlinear load at PCC. It is straightforward to implement because to its ease of design and control capacity. The abnormal load at PCC is fed by control simply while also sending active and reactive power to the grid.Duringimmense sag, LVRT is performed by injecting reactive power in compliance with grid rules.When there is no PV power, the system's use is increased at night by serving as a Distribution STATCOM. These findings explain the production which was tested by simulation and empirically justified on a constructed prototype. The system is governed by several anomalous grid fluctuations. The THD of the grid current is determined to be well within the IEEE-519 standard limits for all of these scenarios.

Parameters:

A. Parameters used in simulation:

Grid voltageeg=125 V, Li=5 mH, Cf=10 μF, Rf=6 Ohms, Voc=627 V, Isc=24.27 A, $Pmpp$=11.4 kW.

REFERENCES:

[1] Vardan Saxena, Nishant Kumar, Bhim
Singh, Bijaya KetanPanigrahi:“Grid integr ated solar PV system during Abnormal condition using IGI”,IEEE Transactions on Electronics,0278-0046, 07 Aug. 2020.

[2] S. Golestan, J.M. Guerrero, J.C. Vasquez, “Single-Phase PLLs: A Review of Recent Advances”, IEEE Trans. Power Elec. , vol. 32, no.12, pp. 9013- 9030, Dec. 2017.

[3] L. Hadjidemetriou, E. Kyriakides, Y. Yang, F. Blaabjerg, “A Synchronization Method for Single-Phase Grid-Tied Inverters”, IEEE Trans. Power Elec., vol. 31, no. 3, pp. 2139-2149, March 2016.

[4] P. Jain, V. Agrawal, B.P. Muni, “Hybrid Phase Locked Loop for Controlling Master-Slave Configured Centralized Inverters in Large Solar Photovoltaic Power Plants”, IEEE. Trans. Ind. App. ,vol. 54, no. 4, pp. 3566-3574, July 2018.

[5] F. Chishti, S. Murshid, B. Singh, “Robust Normalized Mixed-Norm Adaptive Control Scheme for PQ Improvement at

PCC of a RemotelyLocated Wind-Solar PV-BES Mircrogrid", IEEE. Trans. Ind. Infor., vol. 16, no. 3, pp. 1708-1721, March 2020. [6] D. Dong, B. Wen, D. Boroyevich, P. Mattavelli, and Y. Xue, "Analysis of phase-locked loop low-frequency stability in three-phase grid-connected power converters considering impedance interactions," IEEE Trans. Ind. Elect., vol. 62, no. 1, pp. 310–321, 2015.

[7] B. Wen, D. Dong, D. Boroyevich, R. Burgos, P. Mattavelli, and Z. Shen, "Impedance-based analysis of grid-synchronization stability for threephase paralleled converters," IEEE Trans. Power Elect., vol. 31, no. 1, pp. 26–38, 2016.

[8] Q. Chen, X. Luo, L. Zhang, and S. Quan, "Model predictive control for three-phase four-leg grid-tied inverters," IEEE Access, vol. 5, pp. 2834– 2841, 2017.

[9] N. Kumar, B. Singh, and B. K. Panigrahi, "LLMLF-Based Control Approach and LPO MPPT Technique for Improving performance of a Multifunctional Three-Phase Two-Stage Grid Integrated PV System," IEEE Trans. Sust. Energy,vol. 11, no. 1, pp. 371-380, Jan. 2020.

[10] S. Yu, L. Zhang, H. lu, T. Fernando and K.Wong, "A DSE-Based Power System Frequency Restoration Strategy for PV-Integrated Power Systems Considering Solar Irradiance Variations", IEEE Trans. Ind. Inform., vol. 13, no. 5, pp. 2511-2518, Oct. 2017.

[11] V.L. Srinivas, B. Singh and S. Mishra, " Fault Ride-Through Strategy for Two-Stage Grid-Connected Photovoltaic System Enabling Load Compensation Capabilities.", IEEE Trans. Ind. Elec., vol. 66, no. 11, pp. 8913-8924, Nov. 2019.

[12] P. Rodrıguez, A. Luna, R. S. Munoz-Aguilar, I. Etxeberria-Otadui, R. Teodorescu, and F. Blaabjerg, "A stationary reference frame grid synchronization system for three-phase grid-connected power converters under adverse grid conditions," IEEE Trans. Power Elect., vol. 27, no. 1, pp. 99–112, Jan. 2012.

[13] Z. Xin, X. Wang, Z. Qin, M. Lu, P. C. Loh and F. Blaabjerg, "An Improved Second-Order Generalized Integrator Based Quadrature Signal Generator," IEEE Trans. Power Elect., vol. 31, no. 12, pp. 8068-8073, Dec. 2016.

[14] M. Xie, H. Wen, C. Zhu and Y. Yang, "DC offset rejection improvement in single-phase SOGI-PLL algorithms: methods review and experimental evaluation," IEEE Access, vol. 5, pp. 12810-12819, 2017. [15] N. Kumar, I. Hussain, B. Singh, and B. K. Panigrahi, "Implementation of multilayer fifth-order generalized integrator-based adaptive control for grid-tied solar PV energy conversion system," IEEE Trans. Ind. Informat., vol. 14, no. 7, pp. 2857–2868, Jul. 2018.

[16] IEEE Standard for Interconnecting Distributed Resources with Electric Power Systems - Amendment 1, IEEE Std 1547a-2014 (Amendment to IEEE Std 1547-2003), 2014.

[17] Y. Wang, P. Yang, X. Yin and Y. Ma, "Evaluation of low-voltage ridethrough capability of a two-stage grid-connected three-level photovoltaic inverter", in Proc. 17th Int. Conf. Electr. Mach. Syst., 2014, pp. 822-828.

[18] Y. Gui, C. Kim, C.C. Chung, J.M. Guerrero, Y. Guan, J. C. Vasques "Improved Direct Power Control for Grid Connected Voltage Source Converters" IEEE Trans. Ind. Elect., vol. 65, no. 10, pp. 8041-8051, Oct. 2018.

[19] E. Afshari, G.R. Moradi, R. Rahimi, B. Farhangi, Y. Yang, F. Blaabjerg and S. Farhangi, "Control Strategy for Three-Phase Grid Connected PV Inverters Enabling Current Limitation Under Unbalanced Faults", IEEE Trans. Ind. Elec., vol. 64, no. 11, pp. 8908-8918, Nov. 2017.

[20] N. Kumar, V. Saxena, B. Singh and B.K. Panigrahi, "Intuitive Control Technique for Grid Connected Partially Shaded Solar PV Based Distributed Generating System." IET Renewable Power Generation, (Early Access).

[20] K. Choi, S. Kim, S. Jung, R. Kim, " Generalized Switching Modification Method Using Carrier Shift for DC-link Capacitor RMS Current Reduction in Real-Time Implementation", IEEE Trans. Ind. Elect., vol. 66, no. 8, pp. 5992-6001, August 2019.

[22] J. Miret, A. Camacho, M. Castilla, L. G. de Vicuna, and J. Matas, "Control scheme with voltage support capability for distributed generation inverters under voltage sags," IEEE Trans. Power Elect., vol. 28, no. 11, pp. 5252–5263, Nov. 2013. [23] Q. Yan, R. Zhao, X. Yuan, W. Ma, and J. He, "A DSOGI-FLL-based deadtime elimination PWM for three-phase power converters," IEEE Trans. Power Elect., vol. 34, no. 3, pp. 2805–2818, Mar. 2019.

[24] A. Bag, B. Subudhi, P.K. Ray, "An Adaptive Variable Leaky Mean Square Control Scheme for Grid Integration of a PV System", IEEE Trans.Sustainable Energy, (Early Access).